ELEKTRİK, VOL.6, NO.1, 1998, ©TÜBİTAK EMO

Analysis of Nonlinear Sustained Oscillations in Discrete Systems with Backlash and Resolution by Using a Discretization-Oriented Describing Function

M. de la Sen, A. Pena & J. Esnaola
Instituto de Investigaciòn y Desarrollo de Processos IIDP
Dpto. de Electricidad y Electrònica
Facultad de Ciencias
Universidad del Pais Vasco, Leioa (Bizkaia)
Apdo. 644-Bilbao - SPAIN

Abstract

In this paper, a discretization-oriented describing function is derived for nonlinear devices combining backlash and quantization (resolution) while being subject to discretization through a sampler and zero-order hold. Such a describing function is frequency-dependent so that the overall nonlinearity, which includes both resolution and backlash, is interpreted as possessing nonlinear inertia. That nonlinear inertia is generated by the sampling process, since it does not appear if the system is continuous. The presence of nonlinear sustained oscillations (limit cycles) is investigated through simulations.

Keywords: *Backlash, describing function, resolution.*

1. Introduction

Describing function techniques for the analysis of nonlinear devices are based on harmonic linearization (Gibson and Prasanna-Kumar 1961; Gelb and Vander Velde 1974). Their most attractive feature is that they allow the substitution of the nonlinear devices by signal-dependent gains which can be easily introduced in descriptions based on block decompositions in the frequency domain. Several types of describing functions have been derived. For instance, the case of multiple input nonlinearities was discussed in Gelb and Vander Velde (1974), while describing functions were obtained in Taylor (1976) for the case of random inputs. A basic application of such techniques is the determination of self-oscillations through the intersections of the frequency-response hodographs of the linear devices and the critical locus (i.e., the minus inverse of the describing function) of the nonlinear ones in the Nyquist plane (Gelb and Vander Velde 1942; Soto and De la Sen 1984, 1985; Williamson 1976). The linear devices have to be of sufficiently large relative order so that they will be adequate low-pass filters. If the control loop does not possess good low-pass filtering properties, the results can be subject to significant errors when determining self-oscillations (limit cycles) or stability conditions (Bergen et.al. 1982). Those results can be improved by using higher-order harmonic corrections in the describing function (Gibson and Prasanna-Kumar 1961). An additional drawback related to the describing function techniques appears when sampling is used, since sampling introduces in a natural way in the steady-state a displacement of the frequencies as well as their associated higher-order

harmonics appearing in the continuous-time domain. In Dormido and Mellado (1975) and De la Sen and Soto (1984, 1985), an adaptive sampling law based on a sampling criterion of constant amplitude difference (i.e., sampling occurs when the absolute value of the sampled signal varies a prescribed threshold) was studied from a describing function viewpoint. It was shown that the given adaptive sampling law is fully equivalent to a multiple relay with hysteresis. However, the analysis was performed in the continuous-time domain since the overall adaptive sampling law was substituted by the multiple relay with hysteresis because of the equivalence within both physical devices.

The main objective of this paper is to focus on this problem indirectly by including the sampling and hold effect in the shape of the periodic signal used for the analysis of the self-sustained oscillations. *Thus, all the harmonics are included in the analysis prior to the filtering effect of the linear part of the plant.* In the various describing functions, which have been derived in the usual applications, there is a gap related to their applicability to discrete systems. In this paper, the problem of stability and presence of self-oscillations in a system including backlash and resolution (see, for instance, Gibson 1963, Taylor and Lu, 1995, Oldak et.al., 1994) acting on a third-order linear plant is studied under sampling with zero-order hold. The associate *(discretization - oriented) describing function* is obtained by using the output of the zero-order hold as input to the composite (i.e., backlash plus resolution) nonlinearity when its input is periodic. The periodic wave considered for analysis purposes is a *sampled sinusoid under a zero order hold* as a natural way to describe the steady-state behavior. In this way, *the sampling effect is automatically included in the analysis without requiring the use of the extra frequencies generated by the sampling and hold device* that would modify a pure sinusoid (i.e., the fundamental frequency of a self-sustained oscillation in the absence of sampling). Since the describing function is shown to be frequency-dependent, *it is concluded that the sampling process causes a nonlinear inetria*. This technique of analysis minimizes, in addition, the drawbacks that arise from the use of the classical (continuous-time) describing function approach when a long sampling period is used. The linear part of the plant has to possess sufficiently large relative order to attenuate the high-order harmonics. The paper is organized as follows. Section 2 describes the physical process empirically. Section 3 is devoted to obtaining the discretization-oriented describing function for the composite nonlinearity. Numerical simulations are discussed in Section 4, including the case of presence of limit cycles and the results are compared to the real values of those limit cycles obtained from a phase-space numerical investigation of trajectories in the time domain. Finally, conclusions are drawn.

2. Process Description

2.1. Preliminary Heuristical Ideas

Backlash (or mechanical hysteresis) is due to the difference in motion between an increasing and a decreasing output, usually caused by mechanical gearing (see, for instance, Gibson 1963). The two switching surfaces between the backlash and linear zones are the separation surface (Linear zone $\rightarrow$ Backlash zone) and the 'pickup', or recombination surface, (Backlash zone $\rightarrow$ Linear zone). The resolution (quantifier) is shown in Figure 1.a, the backlash is shown in Figure 1.b and the composite of the two with the backlash device in Figure 2. The system is subject to sampling under a zero-order-hold. The trajectory switchings between the linear and backlash zone and vice versa do not occur at the theoretical separation and recombination surfaces but at the next time instants where sampling occurs (i.e., those sampling points located after the continuous switching curves have been crossed). This potential delay in the switching instants between zones is the natural consequence of the presence of the zero-order-hold, which reduces the information in the control

function to that which is available at the sampling instants.

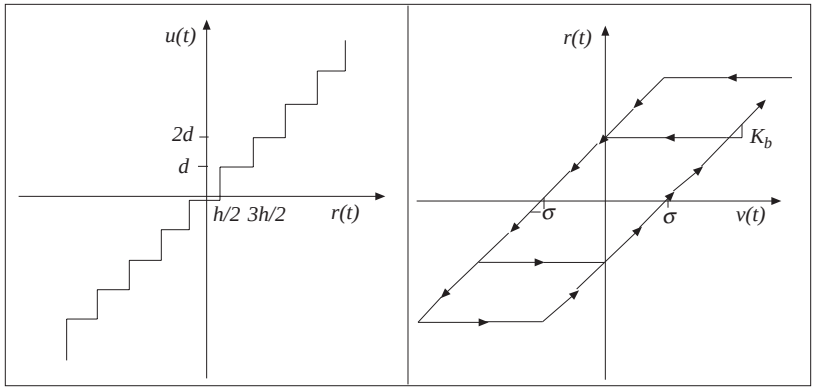

Figure 1. (a) Quantization (Resolution). (b) Backlash

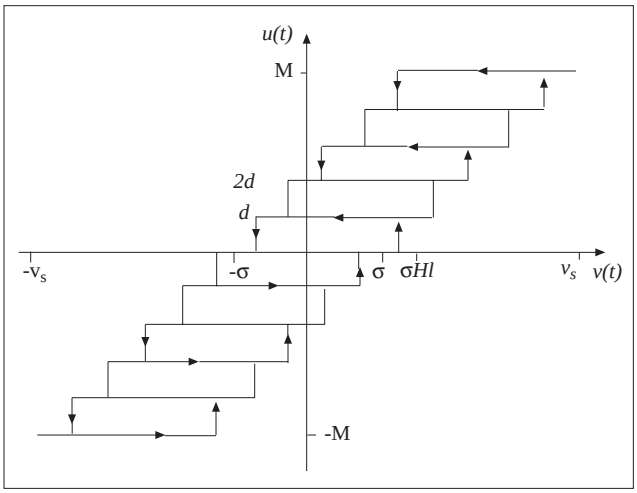

Figure 2. Composite nonlinearity with resolution and backlash.

The composite nonlinearity studied in this paper is that of Figure 2. The overall nonlinear discrete scheme is shown in Figure 3. Its continuous counterpart was studied in Rama and Deekshatulu (1966) for second-order plants so that the associate scheme did not posses either inertia or switching delays caused by sampling. These phenomena are dealt with in this paper and interpreted as being inherent to the sampling and hold process. The role of the zeros in the forward loop is that of modifying both switching surfaces with respect to their counterparts associated with the plant without zeros. This analysis is addressed by incorporating the dynamics of the zeros to the switching process between linear and backlash zones.

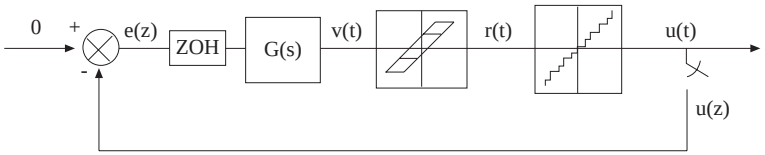

Figure 3. Discrete system with composite nonlinearity and linear plant.

2.2. Finite-State Automaton

The above-mentioned switching delays generating nonlinear inertia are dependent on the a priori switching points on the theoretical switching surfaces of the continuous case, which are obtained in the absence of sampling. As a result, the switching curves between the backlash and linear zones are, in general, time-varying. This means that they can become relocated with different delays at successive intersection points of the phase-trajectory with the theoretical switching surfaces of the continuous case. The motion in the state-space can be described by the four-state automaton of Figure 4.

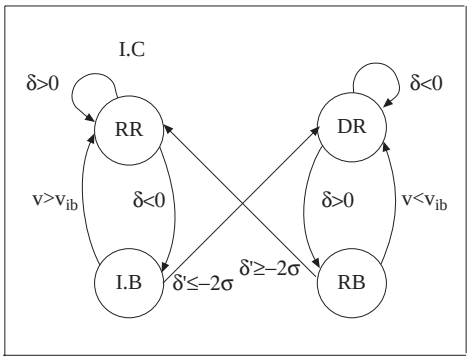

Figure 4. Automaton with the states generated by the composite nonlinearity.

Its four states are:

(I) Rising ramp (RR)

(II) Descendent ramp (DR)

(III) Backlash to the left (LB)

(IV) Backlash to the right (RB)

The motion in backlash zone is described with two states of the automaton to take into account a possible trajectory backlash zone which can occur near the equilibrium. The transitions among automaton states are governed as follows:

(a) The state-space trajectory enters the backlash zones from the rising and descendent ramps when $v'(t) = dv/dt$ (see Figs. 1-2) changes its sign at some $t = kT, k$ being a positive integer and T being the sampling period. For a sufficiently small T, that test can be performed with the sign of the increment $\delta_k = v_{k+1} - v_k$ if a sign change is detected, and then v_{ih} stores v_k.

(b) The trajectory leaves the left backlash zone moving to the descendent ramp if $\delta'_{k+1} = v_{k+1} - v_{ib} \leq -2\sigma$ (σ being the semi-backlash length. See Figs. 1 and 2) and it inverts its motion (backward motion) when $v_{k+1} > v_k$.

(c) The right backlash zone is left if $v_{k+1} < v_{ib}$ (towards the descendent ramp) or if $\delta'_{k+1} \geq 2\sigma$ (towards the rising ramp). Note that all those state transitions occur at sampling points so that *the switching delay causing nonlinear inertia appears as a phenomenon inherent to the discretization process.*

3. Discretization - Oriented Describing Function

3.1. Outputs of the Nonlinearities

Assume that a periodic oscillation exists in the scheme of Figure 3. Neglecting higher-order harmonics, the following equations describe the various parts of the system (see Figures 1-2 for the nonlinearities and the composite nonlinearity) for a short sampling period.

Sampling and Hold Device

$$e(t) = A\sin(\omega t) \ \text{ (prior to sampling and hold)} \tag{1a}$$

$$\begin{aligned} e(t) &= A\sin(\omega t);\ \ e_k = A\sin(\omega kT), \quad \text{for} \quad t = kT, \quad \text{for} \quad t \in [kT, (k+1)T) \\ u(t) &= u_k = u(r(t));\ \ u_k = -A\sin(\omega kT), \quad \text{all} \quad t \in [kT, (k+1)T) \end{aligned} \tag{1b}$$

where A and ω are, respectively, the amplitude and frequency of the fundamental harmonic of the potentially existing tested self-oscillation prior to sampling. $r(t)$ is the backlash function. The fundamental harmonic of the tracking error prior to sampling is $e(t)$, which becomes $\overline{e}(t) = e_k$ after sampling. This sampled signal is in fact used for obtaining the discretization-oriented describing function proposed in this paper.

Backlash Nonlinearity

a) *Linear zone* (i.e., the only nonlinearity in the composite device of Figure 2 is the quantization effect):

$$\begin{aligned} r_k &= K_b[KA\sin(\omega KT) - \sigma\text{sgn}(v_k - v_{k-1})] \\ &= K_b[KA\sin(\omega kT) - \sigma\text{sgn}(\sin(\omega kT) - \sin((k-1)\omega T))] \end{aligned} \tag{2a}$$

where $\text{sgn}(\cdot)$ is the sign function and K and K_b are, respectively, the high-frequency plant gain and the backlash gain in linear zone.

$$r_k = r_{k-1}, \quad \text{if the system was in backlash zone at} \quad t = (k-1)T \tag{2b}$$

b) *Backlash zone*

$$\begin{aligned} r_k &= K_b[v_k - \sigma\text{sgn}(v_k - v_{k-1})], \quad \text{if the system was in linear zone} \\ &\quad \text{at} \quad t = (k-1)T. \end{aligned} \tag{3}$$

The plant input is from Figures 1-3:

$$\begin{aligned} u_k &= D.Int(v_k/h) + (1/2)sgn(v_k)] \\ &= D.Int[KK_bA\sin(\omega kT)/h + (1/2)\text{sgn}(r_k) - \sigma\text{sgn}(v_k - v_{k-1})]. \end{aligned} \tag{4}$$

The subsequent developments are related to the quantization of Figure 1.a and the composite nonlinearity of Figure 2 in the closed-loop system of Figure 3, with extensions for the quantifier of Figure 1.b and a reverse order quantization backlash in the scheme of Figure 3. This alternative scheme can be relevant if the quantifier operates on the output of the linear plant, which occurs, for instance, if a linear controller involving a computer is placed at such a point. In the following, we use sets of sampling points $P_i, Q_i (i = 1, 2)$ to complete the analysis of self-oscillations under a new discretization-oriented describing function. The set $Q = Q_1 \cup Q_2$ is the whole set of samples over one oscillation period of the tentatively searched limit cycle.

Such a set is formed by the disjoint union of indexations for samples of quantified signals corresponding to both the linear and backlash zones on the mechanical backlash plus quantization composite nonlinearity by accounting only once for each set of consecutive samples for which the output of the composite nonlinear device remains constant. Q_1 is the set of samples q_k over one cycle of oscillation in the linear zone such that the output of the composite nonlinearity remains constant over the next $(p_k - 1)$ samples. The meaning of the set Q_2 is similar to that of Q_1 except for the backlash zone. Sets P_1 and P_2 are the number of consecutive samples over which $u_k = u_{q_k}$ in linear and backlash zones, respectively. Since the condition $q_k \in Q_2$ iff $q_k \notin Q_1$ has been imposed, then $Q_1 \cap Q_2 = \emptyset$, i.e., each last sampling point in linear zone preceding the system entrance in backlash zone is considered as a point within backlash zone. These above sets of points are used to compute analytically the proposed describing function in the sequel.

3.2. Describing Function

The describing function of the composite nonlinear characteristics of Figure 2 is calculated by including the sampling effect. It is assumed in the closed-loop scheme of Figure 3 that a steady-state periodic motion exists, the fundamental harmonic of which is assumed to be present in signal $v(t)$, which is parametrized in with its amplitude and frequency. Such a describing function is given, for a periodic input signals in the scheme of Figure 3, by

$$N(\alpha, A, \omega) = q(\alpha, A, \omega) + jq'(\alpha, A, \omega) \tag{5}$$

where j is the imaginary complex unity and α is a parameter related to the nonlinear inertia associated with sampling. The α-parameter establishes a measure of the inertia associated with the sampling effect in the sense that the describing functions are dependent on frequency. *The coefficients of harmonic linearization q and q' are parametrized by the real parameter $\alpha \in [0, 1)$, and are calculated as follows*

$$\begin{aligned} q(\alpha, A, \omega) &= \frac{1}{\pi A}\int_0^{2\pi} u(A\sin(\omega t),\ A\omega\cos(\omega t))\sin(\omega t)d(\omega t) \\ &= \frac{1}{\pi A}\int_\gamma^{2\pi+\gamma} u(A\sin(\omega t), A\omega\cos(\omega t))\sin(\omega t)d(\omega t) \end{aligned} \tag{6a}$$

and, similarly,

$$\begin{aligned} q'(\alpha, A, \omega) &= \frac{1}{\pi A}\int_0^{2\pi} u(A\sin(\omega t), A\omega\cos(\omega t))\cos(\omega t)d(\omega t) \\ &= \frac{1}{\pi A}\int_\gamma^{2\pi+\gamma} u(A\sin(\omega t), A\omega\cos(\omega t))\cos(\omega t))\cos(\omega t)d(\omega t) \end{aligned} \tag{6b}$$

where γ is any real number. Eqns. (6) with (4) lead to

$$\begin{aligned} q(\alpha, A, \omega) &= \frac{1}{\pi A}\left[\sum_{k=0}^{1-1}\left(u_k\int_{\omega(k+\alpha)T}^{\omega(k+\alpha+1)T}\sin\beta d\beta\right) + u_1\int_{\omega(1+\alpha)T}^{2\pi+\omega\alpha T}\sin\beta d\beta\right] \\ &= \frac{D}{\pi A}\left\{\sum_{j\in Q} p_j(Int[(K_1/h)|KA\sin(j\omega T) - \mathrm{sgn}(\sin(j\omega T)\right. \\ &\quad -\sin((j-1)\omega T)|] + 1/2)\mathrm{sgn}[KA\sin(j\omega T) - \sigma(\sin(j\omega T) - \sin((j-1)\omega T))] \\ &\quad \times[\cos((j+\alpha)\omega T) - \cos((j+\alpha+1)\omega T)] \\ &\quad + Int[(K_1/h)(KA\sin((1-j_1)\omega T - \sigma(\sin(j\omega T) - \sin((j-1)\omega T))] \\ &\quad \left.\times[\cos((1+\alpha)\omega T) - \cos(\omega\alpha T)]\right\} \end{aligned} \tag{7a}$$

where $1 = Int[2\pi/(\omega T)]$ and p_k is the number of consecutive times that u_{q_k} is repeated; and

$$q'(\alpha, A, \omega) = \frac{1}{\pi A}\left[\sum_{k=0}^{1-1}\left(u_k \int_{\omega(k+\alpha)T}^{\omega(k+\alpha+1)T} \cos\beta d\beta\right) + u_1 \int_{\omega(1+\alpha)T}^{2\pi+\omega\alpha T} \cos\beta d\beta\right]$$

$$\frac{D}{\pi A}\left\{\sum_{j\in Q} p_j Int[(K_1/h)|KA\sin(j\omega T) - \sigma(\sin(j\omega T) - \sin((j-1)\omega T|] + \frac{1}{2})\right.$$

$$\mathrm{sgn}[KA\sin(j\omega T) - \sigma(\sin(j\omega T) - \sin((j-1)\omega T)][\sin((j+\alpha+1)\omega T)$$

$$-\sin((j+\alpha/\omega T)] + Int[(K_1/h)(KA\sin((1-j_1)\omega T) - \sigma(\sin(j\omega T) - \sin((j-1)\omega T))]$$

$$\left.\times[\sin(\omega\alpha T) - \sin((1+\alpha)\omega T)]\right\}. \tag{7b}$$

Note that in (7) the plant input depends on v and on its time-derivative. This is obvious from the fact that the composite nonlinearity possesses memory due to the presence of backlash.

3.3. Nonlinear Inertia and Limit Cycles

The critical locus associated with the discretization-oriented describing function (5)-(7), i.e., the minus inverse of N, is

$$C(\alpha, A, \omega) = -\frac{1}{N(\alpha, A, \omega)} = -\frac{q(\alpha, A, \omega) - jq'(\alpha, A, \omega)}{q^2(\alpha, A, \omega) + q'^2(\alpha, A, \omega)} \tag{8}$$

which depends on ω (i.e., there exists nonlinear inertia) and it is parametrized in the α-parameter. The amplitude A and frequency ω of possible sustained oscillations (limit cycles) in the scheme of Figure 3 for a linear plant of transfer function $G(s) = B(s)/A(s)$ are given by the intersection of $C(\alpha, A, \omega)$ and $G(j\omega)$ for a given α related to such steady-state-sustained oscillations. The errors in the calculation of ω and A with respect to the real ones increase as the low-pass filtering performances of $G(jw)$ deteriorate (Gibson 1963, Bergen et.al. 1982). Such cycles are stable if, according to Loeb's criterion, $(dG(j\omega)/d\omega \wedge dC(\alpha, A, \omega)/dA)$ is positive. It has been discovered through numerical computation that if $\delta = \omega T < \delta_0 = 12.56 \times 10^{-3}$ or, equivalently, 1 in (7) (i.e., the number of samples per cycle in steady-state) is greater than 500, then the critical locus is, in practice, independent of the α-parameter and the frequency so that $C_0(A) = C(0, A, 0) \approx C(\alpha, A, \omega)$, all $\alpha \in [0, 1)$ and all $\omega \in [0, \delta_0 T^{-1}]$. Thus, the nonlinear inertia can be neglected for $\omega \leq \delta_0 T^{-1}$, namely, for a range of frequency which increases as sampling period T decreases. For $1 < 500$, the critical locus can be considered as dependent on the frequency with this dependence being more relevant as 1 decreases. The critical locus moves to the right as frequency ω increases. If δ is of the order of 50 δ_0 i.e., the number of samples per cycle is of the order of 10, then the dependence of the critical locus becomes apparent. For a limit cycle to exist, the intersection of G and C must be available in the Nyquist plane for all $\alpha \in [0, 1)$ leading to very close values of (ω, A) for any α. That means by trivial frequency-response analysis, that a periodic steady-state mode appears in the closed-loop scheme, which is the standard condition of the existence of oscillation in the continuous-time domain. *Note that in the current context of obtaining discretization-oriented describing functions, the effect of sampling has been included by assuming that the first-order (fundamental) harmonic of the steady-state input to the nonlinear device is a piecewise periodic signal. The step-type discontinuities of that signal appear at sampling instants corresponding to the linear zone of the backlash to include the effect of sampling and hold provided that the linear part of the plant is a low-pass filter that attenuates sufficiently the higher-order harmonics.* In other words, for any distinct $\alpha_1, \alpha_2 \in [0, 1)$, the equations $G(j\omega_1) = C(\alpha_1, A_1, \omega_1)$ and $G(j\omega_2) = C(\alpha_2, A_2, \omega_2)$ have to be satisfied for very close pairs (ω_1, A_1) and (ω_2, A_2). The parameters of the limit cycle (ω, A) [i.e., the frequency

and amplitude of the first harmonic of the sustained oscillation] are calculated with the averages of the intersections $G(j\omega) = C(\alpha, A, \omega)$, all $\alpha \in [0, 1)$. If for a subset of admissible values of α, no intersection exists, then it is claimed that no limit cycle exists since obviously for two close but distinct initial conditions in the state-space, the two trajectories would asymptotically converge to the same sustained oscillation (if any), with this convergence being practically effective, in general, with different initial sampling points (and thus, different values of α), as stated in Section 3.2. In this case, the influence of the nonlinear inertia is very significant. In fact, the influence of N on ω (but not on α) is significant even in the range $1 \in [100, 300]$ while this nonlinear inertia is negligible, as stated before, for $1 > 500$. In the above-mentioned case of 1 being of the order of ten, the loop-filtering properties are poor since the sampling rate is large and higher-order harmonics have large amplitudes. Thus, unsuitable errors can appear in the calculation of limit cycles from the describing function approach.

4. Numerical Examples

4.1. Nonlinear Devices and Sampling Effects

The resolution or quantization and backlash are those of Figures 1-2 with parameters $h = 0.1, d = 0.1, \sigma = 0.2, K_b = 1$ and $v_s = 1.05$. It follows from the discussion of Section 3.3 that for small sampling periods of the order of $10^{-2}, 1 > 500$ in Eqns. (8)-(9) for a range of ω increasing as the sampling period decreases. If T is of the order of 10^{-4}, the critical locus is independent of ω for frequencies increasing up to orders of 10^2, the critical locus being a one-to-one mapping $\omega -> N(A, \omega)$ and the nonlinear inertia being negligible, as shown in Figure 5.a for nonlinearity with and without resolution. As the sampling period increases the nonlinear inertia becomes apparent for larger ranges of frequency, as shown in Figure 5.b. Note in Figure 5.a that the critical locus is serrated in shape due to the resolution action from the comparison of critical locus nonlinearity with and without resolution. Note also that, as input amplitude A increases, the locus tends to be less serrated in shape.

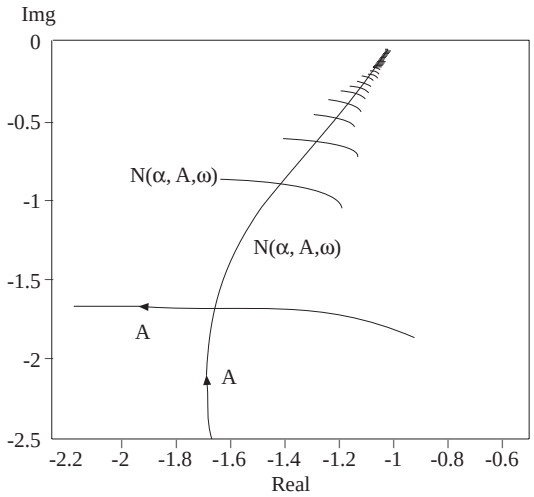

(a)

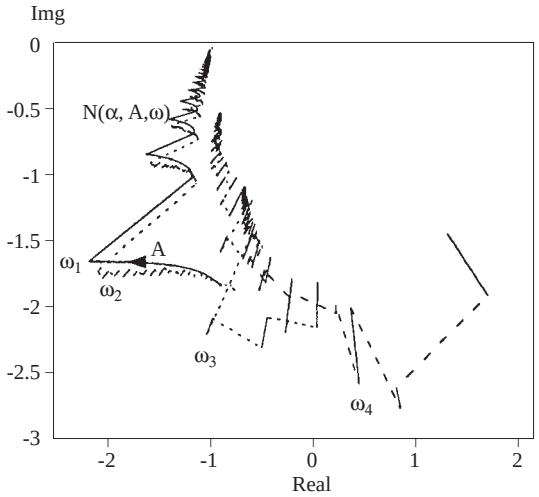

(b)

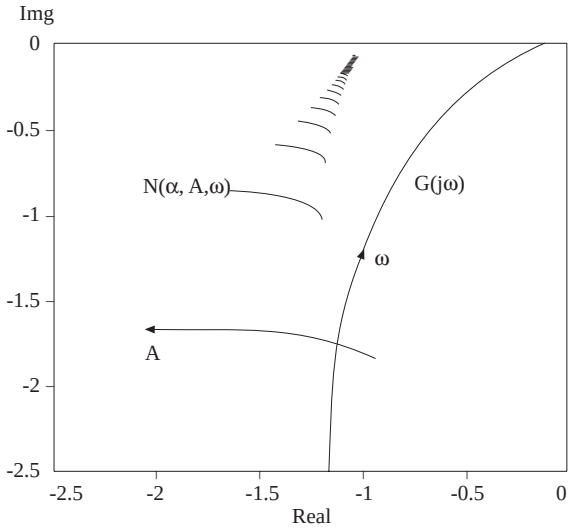

(c)

Figure 5. Discretization-oriented critical locus in the Nyquist plane for, a) the composite nonlinearity and nonlinearity without resolution for $T = 0.0001$ sec.. b) $T = 0.1$ sec., $\omega_1 = 0.1, \omega_2 = 1, \omega_3 = 10$ and $\omega_4 = 20$ rad/sec (nonlinear inertia is relevant).

4.2. Linear Plant

The third-order linear plant has the transfer function

$$G(s) = \frac{K(s + z_1)}{(s + p_1)(s + p_2)(s + p_3)} \tag{9}$$

with the following parameters: $p_1 = 0.1, p_2 = 0.5, p_3 = 2, z_1 = 1.6$ $K = 1$ and T (sampling period) $= 0.01$ sec. The α-parameter is zero in the critical locus unless otherwise stated. A stable limit cycle is detected with $A = 0.258, \omega = 0.530$ rad/sec. The nonlinear inertia for this frequency and the given sampling period is irrelevant (see Section 3.3). The real values obtained from the state-space analysis are $A = 0.257$ and $\omega = 0.529$ rad/sec. Thus, the absolute values of the relative errors in the results are 0.39 % for the amplitude and 0.21 % for the frequency. The intersection of the linear hodograph and the critical locus is shown in Figure 6.a. In Figure 6.b a state-space portrait is shown.

Modification of the Plant Zero. If z_1 is moved to $z_1 = 1$, extensive simulations have shown that the limit cycle disappears. If, at the same time, T increases, new limit cycles do not appear, although the nonlinear inertia becomes important. Thus, the stabilization effect associated with stable zeros is more important, for this class of plants, than the instability associated with high sampling rates in the sense that once a limit cycle has been eliminated by an appropriate choice of the zeros, a possible sampling period increase does not create new limit cycles. It has been found that if z_1 is increased up to $z_1 = 3$, then four stable limit cycles appear.

Modification of the Plant Gain. A gain increase generates a loss in the relative stability, as is well-known even in the linear case. A maximum of four limit cycles can appear if the high-frequency plant gain is increased sufficiently.

Resolution Modification. Limit cycles can disappear when h and d decrease sufficiently while keeping the values of all the remaining parameters if the critical locus of the nonlinearity without resolutio and the hodograph of the linear plant do not have any intersection. This is due to the negligible influence of small quantization in the system, as has been pointed out by Ramu and Deekshatulu (1966) for the continuous case.

Sampling Period and α-Parameter. The calculations deteriorate as T increases, as stated in Section 3.3. The example was also simulated with several sampling rates. Simulation details and graphics were omitted for reasons of space. It is found that for $T = 0.1$ sec. and $(A, \omega) = (0.262, 0.528)$, the parameters of a stable limit cycle of real values are 0.259 and 0.528, respectively. The respective absolute values of the relative errors arising from the method application are 1.2 % for amplitude and 0 % for frequency. For $T = 0.5$ sec., one stable limit cycle is detected with $(A, \omega) = (0.270, 0.520)$. The real values of that limit cycle are 0.269 and 0.524, so that the relative errors between the true values and the computed ones are very small. According to the comments of Section 3.3, the reasons for the increasing errors related to the true registered data are:

- *The sampling period is long and the filtering capability of the plant to the generated (high-amplitude) higher order harmonics is poor. This implies that a first-order harmonic approximation fails to provide good results.*

- *In addition, the number of samples over one input oscillation is very small and the switching delays (with respect to the theoretical switching surfaces) of the current switching surfaces of the discrete problem generate a significant nonlinear inertia.*

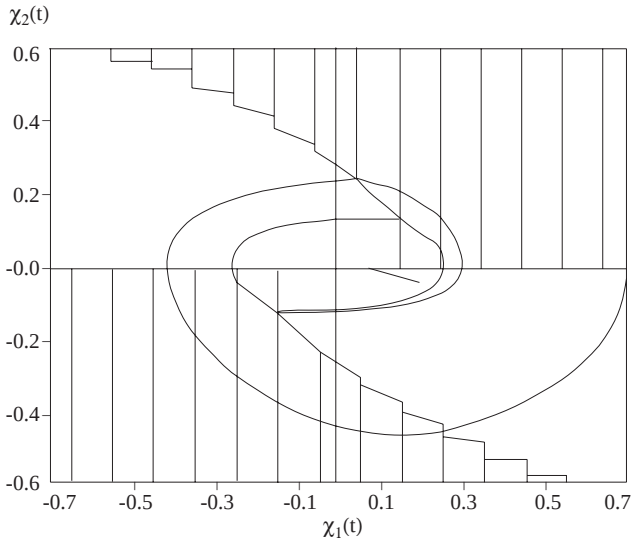

Figure 6. (a) Nyquist plane. Critical locus and Plant hodograph for $T = 0.01$ sec. and $\omega_1 = 0.530$ rad/sec.. b) Time-domain plots for $T = 0.01$ sec.. State-plane for the coordinates $x(t)$ (horizontal) and $dx(t)/dt$ (vertical) with the recombination line and the projection of the stable limit cycle on that plane.

5. Conclusion

A new discretization-oriented describing function has been theoretically obtained and discussed for a composite nonlinear device including both backlash and resolution. Such a describing function, and thus the instantaneous gain of the nonlinear device, is frequency-dependent so that the overall composed nonlinearity described is interpreted as one possessing nonlinear inertia. It has been found that resolution and sampling are instability factors in the sense that limit cycles either appear or increase their frequencies and amplitudes as quantization thresholds and sampling rates become more apparent.

Acknowledgements: The authors are very grateful to DGICYT for its partial support of this study through Project PB96-0257.

References

[1] Gibson, J.E., and Prasanna-Kumar, K.S. 1961. "A new r.m.s. describing function for single-valued nonlinearities", *Proc. I.R.E.*, 1961, **49**, 1321-1326.

[2] Gelb, A. and Vander Velde, W.E., 1974. "Multiple-input describing function and nonlinear system design", (New York: McGraw-Hill).

[3] Bergen, A.R., Chua, L.O., Mees, A.I. and Szeto, E.W., 1982. "Error bounds for general describing function problems", *IEEE Trans. on Circuits and Systems*, Vol.CAS-29, 6, pp.345-354.

[4] Dormido, S. and Mellado, M. 1975. "Determinacion de ciclos limite en sistemas de muestreo adaptativo", *Revista de Informatica y Automatica*, **26**, 4, pp.21-33 (in Spanish).

[5] Gibson, J.E. 1963. *Nonlinear Automatic Control*, (New York: McGraw-Hill).

[6] Ramu, I. and Deekshatulu, B., 1966. "Analysis of systems with backlash and resolution", *Int. J. of Control*, **4**, 4, pp.325-336.

[7] Soto, J.C. and De La Sen, M. 1984. "Non-linear oscillations in nonperiodic sampling systems", *Electronics Letters*, **20**, 20, pp.816-818.

[8] Soto, J.C. and De La Sen, M., 1985. "On the derivation and analysis of a non-linear model describing a class of adaptative sampling laws", *Int. J. of Control*, **42**, 6, pp.1347-1368.

[9] Taylor, J.H., 1976. "Random-input describing functions for multi-input nonlinearities", *Int. J. of Control*, **23**, 2, pp.277-281.

[10] Williamson, D., 1976, "Describing function analysis and oscillations in non-linear networks", *Int. J. of Control*, **24**, 2, pp.283-296.

[11] Taylor, J.H. and Lu, J., 1995. "Robust nonlinear control-system synthesis method for electromechanical pointing systems with flexible mode", *Journal of Systems Eng.*, **5**, 3, pp.192-204.

[12] Oldak, S., Boril, C. and Gutman, P.O., 1994. "Quantitative design of a clas of nonlinear systems with parameter uncertainty", *Int. Journal of Robust and Nonlinear Control*, **4**, 1, pp.101-117.

ELEKTRİK, VOL.6, NO.1, 1998

CONTENTS

An Interoperability Infrastructure for Developing Multidatabase Systems 1
A. DOĞAÇ, G. ÖZHAN, E. KILIÇ, F. ÖZCAN, S. NURAL, S. MANCUHAN, C. DENGİ,
P. KÖKSAL, U. HALICI, B. ARPINAR, C. EVRENDİLEK, V. SADJADİ

Object-Oriented Computer Simulations of Physical Systems Using Dual Reciprocity Boundary Element Methodology 11
J. FRIEDRICH

Performance of Prefiltered Model-Based Frequency Estimators 23
M. A. ALTINKAYA, B. SANKUR, E. ANARIM

Distribution System Planning Usign Mixed Integer Programming 37
B. TÜRKAY

Analysis of Nonlinear Sustained Oscillations in Discrete Systems with Backlash and Resolution by Using a Discretization-Oriented Describing Function 49
M. de la SEN, A. PENA, J. ESNAOLA, F. de CIENCIAS